Thresholds of excitability in three-dimensional dynamical systems

Michal Voslař and Igor Schreiber*
Department of Chemical Engineering and Center for Nonlinear Dynamics of Chemical and Biological Systems, Prague Institute of Chemical Technology, Technická 5, 166 28 Prague 6, Czech Republic
(Received 21 January 2005; published 22 July 2005)

A two-dimensional threshold surface of an excitable system is found as a set of threshold trajectories calculated step by step in cross sections of the phase space. The method leads to a highly nonlinear boundary value problem that can be solved numerically with the use of adaptive multiple shooting and continuation methods. We demonstrate this technique by examining a model of a biochemical oscillator with two positive feedbacks. Generalization to arbitrary dimension is discussed.

DOI: 10.1103/PhysRevE.72.016216 PACS number(s): 05.45.−a, 82.20.Wt

INTRODUCTION

Excitability represents a basic mechanism for recognition and adequate response to external stimuli. In general, excitable systems are nonlinear systems with a stable steady state that are able to respond to a suitable small superthreshold perturbation (signal) by a relatively large-amplitude transient oscillation. The existence of the threshold makes it possible to discern the signal from ordinary noise, while sufficient amplification is a precondition for effective processing of the response. Therefore excitability is frequently met when studying living organisms on various levels of complexity, from ecology [1] to physiology [2,3] and to biochemistry [2–4]. There are also many examples of nonbiological systems that display excitability [5–8].

In this work we focus on cases described by ordinary differential equations. A basic qualitative explanation of excitability and related notions applied to a general two-variable dynamical system was presented in Ref. [9] where a relationship between the threshold set and a middle part of the nullcline for the autocatalytic variable is formulated. Other approaches appeared, such as those employing isochrones [10]. However, none of these studies treat the excitability as a quantitative property, which exists only in a bounded region of the parameter space. In addition, the study of excitability has been so far restricted to two variables.

A well-studied case of excitability is associated with three coexisting steady states, one of them being stable, where the threshold is determined by a stable separatrix of the saddle [11]. In the parameter space, such excitability is usually suppressed in favor of bistability. A more frequent case is an excitable system with a unique steady state, which is often associated with a large parameter domain near a subcritical Hopf bifurcation. For an outside observer the difference between both types is virtually undetectable but the threshold in the latter case eludes a simple description. For two-variable systems, a formulation of the threshold is found in our previous work [12,13]. Here we present an extension to three-variable systems where topologically new phenomena can be expected. The method is applied to a well-known model of two consecutive enzyme-catalyzed reactions with positive feedback [14].

THEORY

The strategy for calculations in a three-dimensional system is based on the same principles as the previously thoroughly examined two-dimensional case [13]. Let us consider a dynamical system described by a set of ordinary differential equations

$$\frac{d\boldsymbol{x}}{dt} = \mathbf{v}(\boldsymbol{x}), \quad \boldsymbol{x} \in R^n, \tag{1}$$

which has a unique stable steady state $\boldsymbol{x}_S$ satisfying condition

$$\mathbf{v}(\boldsymbol{x}_S) = \mathbf{0}. \tag{2}$$

As implied by the qualitative definition of excitable dynamics introduced above, the excitable system must, apart from displaying the threshold set, be able to amplify any superthreshold signal. We treat the threshold set $\mathcal{T}$ as a smooth codimension one surface in the phase space made up of negatively directed semiorbits of Eq. (1) [13], which are locally strongly repelling so that response to any subthreshold perturbation becomes rapidly damped, while response to any superthreshold perturbation winds around $\mathcal{T}$ and thus amplifies the signal. First, we need to define the size of the perturbation and the response. By perturbation we understand an instantaneous deviation from the steady state caused externally. For the amplitude of either the perturbation or the response we have

$$A = \|\boldsymbol{x} - \boldsymbol{x}_S\| = \sqrt{\sum_{i=1}^{n} (x_i - x_{Si})^2}. \tag{3}$$

Upon the perturbation, $\boldsymbol{x}$ evolves in time according to Eq. (1), and so does A. For an excitable system there is a region in the phase space where A increases with time because trajectories locally depart from $\boldsymbol{x}_S$. The boundary of this region corresponds to a condition for trajectories to be locally nearest or most distant, which is a hypersurface of codimension one satisfying

*Electronic address: Igor.Schreiber@vscht.cz

$$f = \mathbf{v}(\boldsymbol{x})(\boldsymbol{x} - \boldsymbol{x}_S) = 0, \tag{4}$$

where for the locally nearest point of an observed piece of trajectory we set $\boldsymbol{x}=\boldsymbol{x}_L$ and for the most distant point we set $\boldsymbol{x}=\boldsymbol{x}_R$. Eq. (4) thus represents a unified formulation for both the left and right boundary condition. By substituting $\boldsymbol{x}_L$ or $\boldsymbol{x}_R$ satisfying Eq. (4) for $\boldsymbol{x}$ in Eq. (3) we obtain for a given orbit a minimal size of the perturbation P, or a maximal amplitude of the response R, respectively. It is convenient to take a relative amplification

$$r = \frac{R - P}{P} \tag{5}$$

as a characteristic of the given trajectory. In addition, we need to evaluate a separation rate

$$\frac{dr}{dP} = \frac{\text{grad } r\, \boldsymbol{d}^0}{\text{grad } P\, \boldsymbol{d}^0}, \tag{6}$$

where grad$=d/d\boldsymbol{x}_L$, and $\boldsymbol{d}^0$ is a normalized vector tangent to the hypersurface defined by Eq. (4) evaluated at $\boldsymbol{x}_L$. If $n=2$, this hypersurface is simply a curve, which makes the calculations for two-variable systems viable [13]. For $n>2$, $\boldsymbol{d}^0$ is not unique and additional constraints must be employed as shown below.

To locate the threshold, we need to find orbits with the highest possible separation rates. Equation (2) can be presolved to yield $\boldsymbol{x}_S$. Taking into consideration that $\boldsymbol{x}_R$ is the end point of a solution of Eq. (1) with the initial point $\boldsymbol{x}_L$ for an unknown time T, Eq. (1) subject to boundary conditions according to Eq. (4) represents a boundary value problem for $n+1$ unknowns $\boldsymbol{x}_L$ and T. This problem is well-defined only for $n=2$, since Eq. (4) represents only two boundary conditions. It can be solved by numerical continuation [15] combined with shooting method. Due to extreme instability of the orbits, adaptive multiple shooting is necessary [16]. We obtain a family of trajectory segments from $\boldsymbol{x}_L$ to $\boldsymbol{x}_R$ parametrized by T. If we calculate, at each continuation step, the characteristic amplification r, and the separation rate dr/dP, we can determine a single trajectory representing the excitation threshold according to the selection conditions

$$\frac{dr}{dP} \text{ is max} \quad \text{and} \quad r \geqslant 1. \tag{7}$$

Now we show, how the above approach needs to be modified, when the dimension of the phase space $n=3$. While for $n=2$ the threshold set was simply formed by a piece of a single trajectory satisfying conditions (7), in the three-variable system the threshold set is a surface made up of pieces of individual threshold trajectories. The basic idea is to choose in the 3D phase space a convenient axis and a plane containing this axis, which is rotated. If we restrict the direction of perturbation to this plane, we can find one of the trajectories making up the threshold set in the same fashion as in the two-variable case. By repeating the calculations for the plane sequentially rotated about the chosen axis, we can obtain a family of trajectory pieces that jointly represent the threshold surface. Thus Eqs. (1)–(7) remain valid, likewise, the calculation of grad r and grad P, described in detail in [13], is unchanged. By restricting the perturbation to a plane, the missing third boundary condition is given and, simultaneously, this also provides the so far incomplete determination of the normalized tangent vector $\boldsymbol{d}^0$.

Although the axis of rotation can in principle be chosen arbitrarily, it is convenient to associate it with the autocatalytic variable. Let us assume that the autocatalytic species is the kth variable and define a planar cross-section ρ containing a rotation axis that is parallel to the kth coordinate axis and passes through $\boldsymbol{x}_S$. A normal equation for ρ employing directional angles α_i, α_j, α_k [17] leads to

$$(x_{Li} - x_{Si}) \cos \alpha_i + (x_{Lj} - x_{Sj}) \sin \alpha_i = 0, \tag{8}$$

where the term for k vanishes and the two remaining directional angles are expressed in terms of α_i, which represents a parametrized rotation of ρ.

Now we can calculate the vector $\boldsymbol{d}^0$ occurring in Eq. (6) as follows:

$$\boldsymbol{d}^0 \text{ grad } f(\boldsymbol{x}_L) = 0, \quad \|\boldsymbol{d}^0\| = 1, \tag{9}$$

$$d_i^0 \cos \alpha_i + d_j^0 \sin \alpha_i = 0. \tag{10}$$

Equations (9) remain the same as in the two-variable case [13], while Eq. (10) restricts $\boldsymbol{d}^0$ to the cross-sectional plane ρ.

A starting point for numerical calculations requires Eq. (2) to be solved for $\boldsymbol{x}_S$; an initial trajectory segment is found by integrating Eq. (1) and searching for points $\boldsymbol{x}_L$ and $\boldsymbol{x}_R$ satisfying Eq. (4). In this way we also find T, and by using Eq. (8) we calculate the rotation angle α_i. Then the adaptive-grid multiple shooting method combined with continuation is employed [15,16]. By repeating continuations successively with respect to T and α_i, all the orbits belonging to a threshold surface are calculated. If $\boldsymbol{x}_S$ is a focus, then $\boldsymbol{x}_L$ and $\boldsymbol{x}_R$ may not be unique and global extremes should be used. This feature leads to a highly curved threshold $\mathcal{T}$ with several loops around $\boldsymbol{x}_S$.

MODEL

As a test example we chose a model of two successive enzyme reactions, each with a positive feedback, due to Decroly and Goldbeter [14]. It is a prototype of a simple biochemical oscillator providing a number of periodic regimes, as well as chaos and bistability between a steady state and periodic oscillations [14]. Excitability has not yet been examined. The original model is slightly recast to keep the same scale for all three variables:

$$\frac{dx_1}{dt} = v - \sigma_1 \phi(x_1, x_2), \tag{11}$$

$$\frac{dx_2}{dt} = q_1 q_2 \sigma_1 \phi(x_1, x_2) - \sigma_2 \eta(x_2, x_3), \tag{12}$$

$$\frac{dx_3}{dt} = \sigma_2 \eta(x_2, x_3) - k_s x_3, \tag{13}$$

where x_1, x_2, and x_3 are dimensionless concentrations of a substrate and two self-activating products, respectively, and

$$\phi(x_1,x_2) = \frac{x_1(1+x_1)(1+x_2/q_2)^2}{L_1 + (1+x_1)^2(1+x_2/q_2)^2}, \tag{14}$$

$$\eta(x_1,x_2) = \frac{x_2(1+x_3)^2}{L_2 + (1+x_3)^2} \tag{15}$$

Control parameters v and k_s represent the inlet rate of the substrate and the rate of removal of the second product, respectively. The values of other parameters taken from [14] are $q_1=50$, $q_2=0.02$, $\sigma_1=10\ s^{-1}$, $\sigma_2=10\ s^{-1}$, $L_1=5\times10^8$, and $L_2=100$.

RESULTS

A bifurcation diagram in v and k_s displays three separate regions of a unique excitable stable steady state separated from a common oscillatory region by Hopf bifurcation curves [14]. Dynamics in two regions, where excitability is quite distinct and well developed, are discussed below.

First we set $v=6\ s^{-1}$ and $k_s=0.2\ s^{-1}$, which is well away from the Hopf bifurcation curve on the stable steady state side. A superthreshold perturbation of the steady state $\boldsymbol{x}_S$ is achieved by decreasing the concentration of the first product x_2 to about one third of its steady state value. An inhibitory process depleting x_2 and x_3 is initiated, followed later by an autocatalytic recovery of both species—this is an example of *inhibitory excitability* [13]. We choose the plane of perturbations satisfying Eqs. (4) and (8) to be parallel with the x_3 axis (i.e., $k=3$) and its rotation angle is measured with respect to the x_1 axis (i.e., $\alpha_i=\alpha_1$). Figure 1 shows a set of response trajectories to perturbations with varying size calculated for a fixed value of $\alpha_1=0.7156$. The one that satisfies the threshold condition (7) belongs to the threshold surface, which is then obtained successively as α_1 is varied. The surface is curved along trajectories and nearly linear in the x_1 direction indicating that this case is a simple three-dimensional analog of excitable dynamics found in two-variable systems.

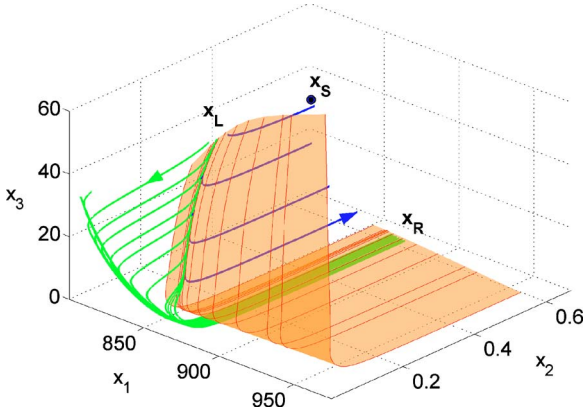

FIG. 1. (Color online) Phase portrait showing superthreshold (green/light) and subthreshold (blue/dark) trajectories for a particular cross section given by $\alpha_1=0.7156$, and a set of threshold trajectories (thin red/medium-dark lines) for varying α_1 forming the entire threshold surface (ocher/light); control parameters: $v=6\ s^{-1}$; $k_s=0.2\ s^{-1}$.

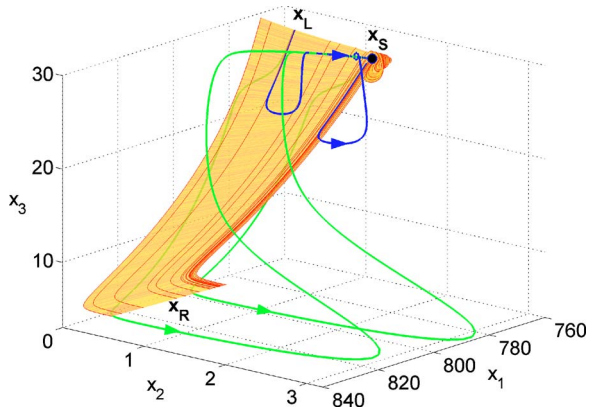

FIG. 2. (Color online) Threshold surface and two pairs of superthreshold (green/light) and subthreshold (blue/dark) trajectories at $v=4.8\ s^{-1}$ and $k_s=0.2\ s^{-1}$.

Now we set the control parameters at $v=4.8\ s^{-1}$ and $k_s=0.2\ s^{-1}$ so that the system is shifted to a close vicinity of the Hopf bifurcation. The steady state, which was originally a node becomes a focus-node and the excitability becomes stronger in the sense that superthreshold perturbations are possible in virtually any direction, because the threshold set forms a highly curved funnel that nearly surrounds the steady state; see Fig. 2.

A different type of excitable behavior is found within the second region of excitable steady states as shown in Fig. 3. For parameter values $v=0.8\ s^{-1}$ and $k_s=5\ s^{-1}$ the threshold surface is marked by a sharp decrease in x_3 immediately after the perturbation followed by increase in x_1, and its limited extent is due to the inequality part of (7). Separating properties of the threshold set become visible during the phase of the increase in x_1 as indicated by a subthreshold and a superthreshold trajectory. Upon leaving the vicinity of the threshold, the trajectories undergo a long oscillatory transient before settling onto the steady state. There are two oscillatory modes, large-amplitude oscillations and small-amplitude ones near the focal steady state. The superthreshold trajectories possess about twice as many large oscillatory loops as

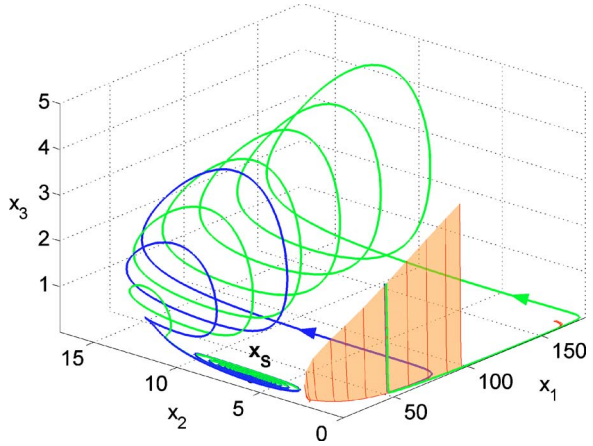

FIG. 3. (Color online) Threshold surface, a superthreshold (green/light) and a subthreshold (blue/dark) trajectory at $v=0.8\ s^{-1}$ and $k_s=5\ s^{-1}$.

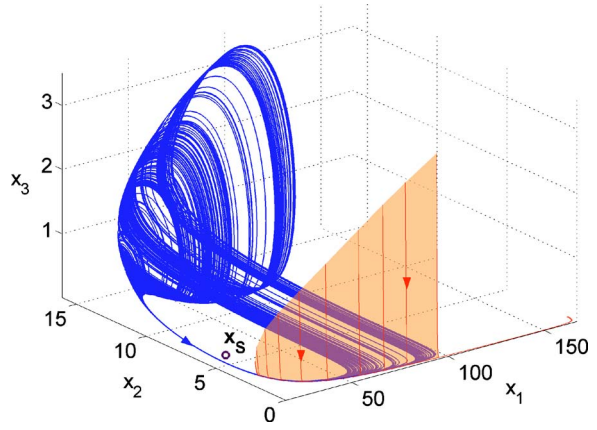

FIG. 4. (Color online) Chaotic attractor at $v=0.658\ \mathrm{s}^{-1}$ and $k_s=5\ \mathrm{s}^{-1}$ bounded by the threshold surface.

the subthreshold ones because of the strong separation. The threshold set helps to characterize dynamics on a chaotic attractor found in the adjacent parameter space across the Hopf bifurcation at $v=0.658\ \mathrm{s}^{-1}$ and $k_s=5\ \mathrm{s}^{-1}$. In Fig. 4 the threshold surface $\mathcal{T}$ is calculated with respect to the now unstable steady state. Any orbit on the chaotic attractor approaches $\mathcal{T}$ from one side and subsequently is repelled while staying on the same side. In fact, the exponential divergence on the attractor is entirely due to the presence of $\mathcal{T}$. This feature is related to T-repellers [10]. Moreover, random noise will divert some orbits to the other side of $\mathcal{T}$ and cause expansion of the attractor.

DISCUSSION

The proposed method of determining threshold surfaces in three-dimensional excitable dynamical systems is an extension of our earlier work on two-variable systems [13]. By restricting the amplitude P of the perturbation to a suitably chosen cross-sectional 2D plane we can find one threshold trajectory. Rotation of this plane about a convenient axis parametrized by an angle α then allows for finding the entire threshold surface. This approach can be formally extended to dynamical systems with any dimension. For instance, in a four-variable system, the threshold set is a three-dimensional hypersurface. As before, we can choose a codimension one hyperplane rotating about an axis parametrized by α. Within this three-dimensional hyperplane, another axis defines rotation of a two-dimensional plane parametrized by an angle β. Thus by fixing α and β, a single threshold trajectory is found so that the constraint (7) is satisfied and the entire threshold set is obtained by successively sweeping both angles. However, the transition from two- to three-variable systems is the most important step, because it represents a major change in topology allowing for occurrence of phenomena associated with excitability such as bursting and chaos.

The approach outlined above was tested for sensitivity to the choice of the rotation axis of the cross section. The presented results were systematically done for two choices: the axis parallel to x_1 and the axis parallel to x_3; we also performed some tests with the axis parallel to x_2. All these calculations provided the same results. As with two-variable systems [13], our approach makes also possible studies of parameter dependence of the threshold sets and their disappearance causing the excitability to vanish.

ACKNOWLEDGMENTS

Authors acknowledge support from the Czech Science Foundation, Grant Nos. 203/02/D051 and 203/03/0488, and from the Czech Ministry of Education, Grant No. MSM6046137306.

[1] J. D. Murray, *Mathematical Biology* (Springer-Verlag, Berlin, 1989).
[2] D. J. Aidley, *The Physiology of Excitable Cells* (Cambridge University Press, Cambridge, UK, 1998).
[3] J. Keener and J. Sneyd, *Mathematical Physiology* (Springer-Verlag, New York, 1998).
[4] *Computational Cell Biology*, edited by C. P. Fall *et al.* (Springer-Verlag, New York, 2002).
[5] J. Zagora, M. Voslař, L. Schreiberová, and I. Schreiber, Phys. Chem. Chem. Phys. **4**, 1284 (2002).
[6] M. Dolník and I. R. Epstein, J. Chem. Phys. **97**, 3265 (1992).
[7] S. P. Dawson, M. V. D'Angelo, and J. E. Pearson, Phys. Lett. A **265**, 346 (2000).
[8] B. Krauskopf *et al.*, Opt. Commun. **215**, 367 (2003).
[9] J. C. Alexander, E. J. Doedel, and H. G. Othmer, SIAM J. Appl. Math. **50**, 1373 (1990).
[10] A. Rabinovitch and I. Rogachevskii, Chaos **9**, 880 (1999).
[11] W. D. McCormick, Z. Noszticzius, and H. L. Swinney, J. Chem. Phys. **94**, 2159 (1991).
[12] J. Zagora, M. Voslař, L. Schreiberová, and I. Schreiber, Faraday Discuss. **120**, 313 (2001).
[13] M. Voslař and I. Schreiber, Phys. Rev. E **69**, 026210 (2004).
[14] O. Decroly and A. Goldbeter, Proc. Natl. Acad. Sci. U.S.A. **79**, 6917 (1982).
[15] M. Marek and I. Schreiber, *Chaotic Behavior of Deterministic Dissipative Systems* (Cambridge University Press, Cambridge, UK, 1995).
[16] M. Kohout, I. Schreiber, and M. Kubíček, Comput. Chem. Eng. **26**, 517 (2002).
[17] H. J. Bartsch, *Mathematische Formeln* (VEB Fachbuchverlag, Leipzig, 1977).